

Plasmonic detector/spectrometer of subterahertz radiation based on two-dimensional electron system with embedded defect

V. M. Muravev and I. V. Kukushkin

Citation: *Appl. Phys. Lett.* **100**, 082102 (2012); doi: 10.1063/1.3688049

View online: <http://dx.doi.org/10.1063/1.3688049>

View Table of Contents: <http://apl.aip.org/resource/1/APPLAB/v100/i8>

Published by the [American Institute of Physics](#).

Related Articles

Ultra-low-noise MoCu transition edge sensors for space applications

J. Appl. Phys. **109**, 084507 (2011)

YBa₂Cu₃O_{7- δ} quasioptical detectors for fast time-domain analysis of terahertz synchrotron radiation

Appl. Phys. Lett. **98**, 043504 (2011)

Low noise and wide bandwidth of NbN hot-electron bolometer mixers

Appl. Phys. Lett. **98**, 033507 (2011)

Thicker, more efficient superconducting strip-line detectors for high throughput macromolecules analysis

Appl. Phys. Lett. **98**, 023702 (2011)

Readout-power heating and hysteretic switching between thermal quasiparticle states in kinetic inductance detectors

J. Appl. Phys. **108**, 114504 (2010)

Additional information on *Appl. Phys. Lett.*

Journal Homepage: <http://apl.aip.org/>

Journal Information: http://apl.aip.org/about/about_the_journal

Top downloads: http://apl.aip.org/features/most_downloaded

Information for Authors: <http://apl.aip.org/authors>

ADVERTISEMENT



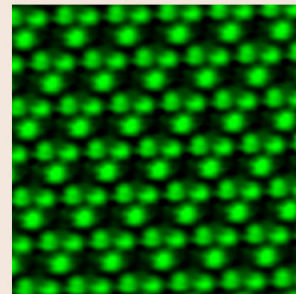
**ASYLUM
RESEARCH**
The Technology Leader in SPM/AFM

Register Now at
www.asylumresearch.com

Free AFM Webinar February 22 Register Now

“Smaller and Quieter: Ultra-High Resolution AFM Imaging”

With Jason Cleveland, AFM pioneer,
inventor and Asylum Research co-founder



Plasmonic detector/spectrometer of subterahertz radiation based on two-dimensional electron system with embedded defect

V. M. Muravev^{1,2,a)} and I. V. Kukushkin^{1,2}

¹*Institute of Solid State Physics, RAS, Chernogolovka 142432, Russia*

²*Terasense Development Labs, Chernogolovka 142432, Russia*

(Received 16 November 2011; accepted 3 February 2012; published online 21 February 2012)

We demonstrate that the introduction of a defect in the form of an electron density step into a two-dimensional electron system (2DES) locally rectifies the alternating potential of plasma waves. The rectification mechanism is active at temperatures up to room temperature. We observe photovoltage oscillations in a back-gated 2DES with a density defect, when tuning the density under incident subterahertz radiation. The oscillations originate from the interference of 2D plasma waves excited by subterahertz radiation. The period of oscillations depends on the radiation wavelength. These phenomena can be exploited further to produce detectors/spectrometers for millimeter waves. © 2012 American Institute of Physics. [doi:10.1063/1.3688049]

Detection and spectroscopy of millimeter and sub-millimeter electromagnetic radiation (100 GHz-3 terahertz (THz)) remain a challenging problem in applied physics. In part, such interest is caused by the unique properties of THz radiation, which predestine potential applications in the fields of communication, imaging, medical diagnosis, and chemical and biological sensing, as well as in security and quality-control applications.¹ The bandwidth of conventional semiconductor transistors does not exceed 50 GHz, rendering them unfit for THz applications. One approach to circumvent this restriction in bandwidth is to transform incident THz electromagnetic radiation into plasma waves propagating in the transistor channel. Devices constructed using this approach operate at much higher frequencies than conventional transit-time limited devices, because the plasma waves propagate much faster than electrons. Moreover, owing to the classical nature of plasma excitations, plasmonic devices may function even at room temperature. The main challenge for plasmonic devices is to be able to efficiently rectify the alternating potential of plasma excitation into detectable *dc* photovoltage. One of the possible rectification mechanisms involves using the hydrodynamic nonlinearity of plasma waves restricted to a stripe of two-dimensional electrons with different boundary conditions.²⁻⁴ Another scenario involves rectification by using the nonlinear behaviour of the contacts.^{5,6} In this letter, we report on the efficient local rectification of plasma waves by introducing a nonlinear defect into a two-dimensional electron system (2DES). Devices with such nonlinear elements can be used as plasmonic on-chip detectors/spectrometers of subterahertz radiation.

All samples were fabricated from the commercially available GaAs/AlGaAs heterostructures. We used two types of heterostructures A and B for the experiments. The type A of structure had an 18 nm single quantum well located 135 nm below the crystal surface. A n^+ GaAs back-gate was grown *in-situ* at a distance d of 765 nm below the quantum well. The electron density n_s was tuned by applying a volt-

age to the back-gate. The density was varied from $1 \times 10^{11} \text{ cm}^{-2}$ to $5 \times 10^{11} \text{ cm}^{-2}$ and the mobility ranged between $1 \times 10^6 \text{ cm}^2/\text{Vs}$ and $5 \times 10^6 \text{ cm}^2/\text{Vs}$ for these densities ($T = 4.2 \text{ K}$). Structures of the type B did not have a back-gate. They comprised a single heterojunction with an electron density of $n_s = 1.6 \times 10^{11} \text{ cm}^{-2}$ or $n_s = 4.6 \times 10^{11} \text{ cm}^{-2}$ and mobility of $1 \times 10^6 \text{ cm}^2/\text{Vs}$. The sample was placed in an oversized 16 mm waveguide. A set of backward wave oscillators operating in the frequency range of 40 to 200 GHz were used to illuminate the sample with continuous wave radiation. The radiation was modulated at a frequency of 1 kHz. The photovoltage was then detected at the modulation frequency with a lock-in amplifier. The device consists of a stripe of the 2DES with a length of 1.5 mm and width W of $50 \mu\text{m}$ and terminates at each end in an ohmic contact referred to as the source or drain (inset of Fig. 1). The stripe was covered by two front gates $G1$ and $G2$, which define the plasmonic resonator of length L . Devices with L of 100 and $20 \mu\text{m}$ were investigated.

Figure 1(a) shows typical traces of the photovoltage signal as a function of the electron density for three different subterahertz frequencies. The photovoltage is measured between the source and the drain contacts for the device with the plasmonic resonator length $L=100 \mu\text{m}$ when the 2DES region under $G1$ is partially depleted to the density $n_1 = 1 \times 10^{11} \text{ cm}^{-2}$. The traces have been offset vertically for clarity; the arrows indicate the zero signal level in the absence of radiation incident on the sample. In each trace, a series of oscillations are observed. We assert that the maxima originate from the constructive interference of plasma waves with wave numbers $q = N\pi/L$. The plasma waves are restricted by gates $G1$ and $G2$ to the plasmonic resonator region. Here, N is an odd integer. According to the dipole approximation, homogeneous incident radiation can only excite modes with odd values of N .⁷ The subterahertz radiation couples to the metallic gates and triggers plasma waves in the 2DES. The 2DES regions near the gates represent a step in the plasmon dispersion, providing a strong reflection of plasma waves. This efficiently confines the plasma waves to the plasmonic resonator. By applying a depletion voltage

^{a)}Author to whom correspondence should be addressed. Electronic mail: muravev_vm@mail.ru.

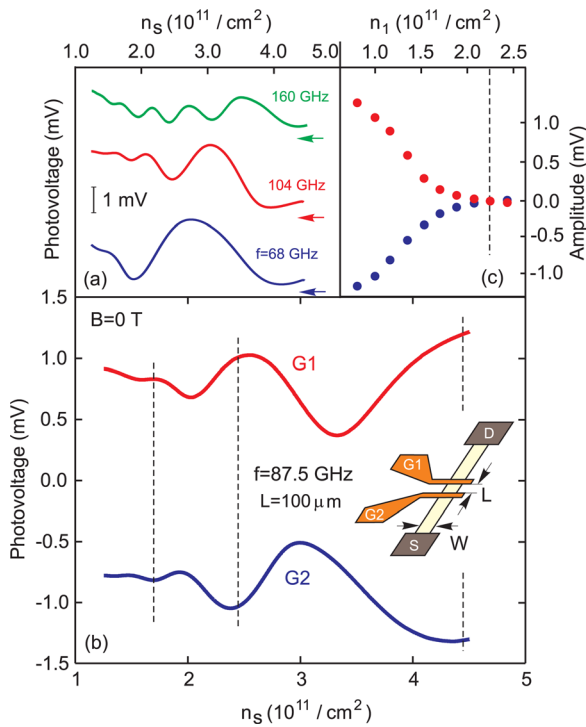


FIG. 1. (Color online) (a) Photovoltage signal as a function of electron density in the presence of 68, 104, and 160 GHz radiation. The curves are offset vertically for clarity. (b) Photovoltage oscillations for $f = 87.5$ GHz when a depletion voltage is applied to gate G1 (top curve) or gate G2 (bottom curve). The inset shows a schematic view of the device geometry. (c) Dependence of dc -photovoltage amplitude on density step at the rectification defect. The device temperature was $T = 4.2$ K and structure type A.

to one of the gates, we introduce a defect into the 2DES in the form of an electron density step. This defect rectifies the ac plasmon potential from one side of the resonator to dc -photovoltage. This outlined device operation picture is corroborated in the remainder of the manuscript.

Plasma waves in the 2DES, sandwiched between an AlGaAs layer of thickness d_1 at the top and an AlGaAs layer of thickness d followed by a conducting back-gate at the bottom, have the following plasma spectrum in the limit of $qd \ll 1$ and $qd_1 \ll 1$:^{8,9}

$$\omega_p(q)^2 = \frac{n_s e^2 d}{m^* \epsilon \epsilon_0} q^2. \quad (1)$$

Here, n_s and m^* denote the density and the effective mass of the two-dimensional (2D) electrons, whereas ϵ_0 and ϵ denote the permittivities of the vacuum and GaAs, respectively. The densities at which maxima occurred in the photovoltage (Fig. 1(a)) are precisely described by Eq. (1). The photovoltage oscillations in Fig. 1(a) vary with the frequency of the incident radiation. We found that their periodicity $\Delta(1/\sqrt{n_s})$ is inversely proportional to the subterahertz frequency f . Hence, the device may serve as a “spectrometer-on-a-chip.”

Figure 1(b) shows how the position of the defect with respect to the plasmon resonator influences the device response. The upper curve corresponds to the case when only defect G1 is present, that is, a depletion voltage is applied only to gate G1. This voltage corresponds to an electron concentration of $n_1 = 1 \times 10^{11}/\text{cm}^2$ in the defect region. The bottom curve corresponds to the case when a depletion volt-

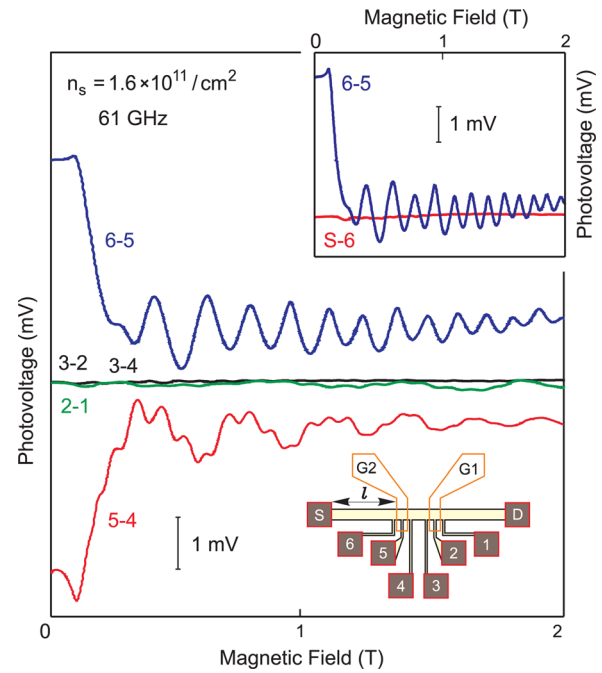


FIG. 2. (Color online) Photovoltage oscillations when sweeping the magnetic field measured from different pairs of potential probes connected to various parts of the device. Depletion voltage is applied to gate G2. The data were recorded for the structure type B with $n_s = 1.6 \times 10^{11}/\text{cm}^2$. The plasmon rectification spatially occurs at the defect electron density step. A sketch of the device under study is shown. The inset demonstrates that nonideal contact characteristics do not contribute significantly to the observed photovoltage.

age is applied only to gate G2. The asymmetry of the curves with respect to zero signal level indicates that we can independently control the plasmon rectification on each side of the resonator. The amplitude of the observed photovoltage oscillations depends strongly on the defect density step ($n_s - n_1$). Figure 1(c) shows the photovoltage recorded as a function of the density step for a fixed resonator electron density of $n_s = 2.3 \times 10^{11}/\text{cm}^2$ and a radiation frequency of $f = 87.5$ GHz. The high-frequency nonlinearity of the defect starts from zero at $n_1 = n_s$ and reaches the maximum for $n_1 \approx 0.7 \times 10^{11}/\text{cm}^2$, when the region under the rectification gate is totally depleted. We found that the observed plasmon nonlinearity can be caused by any local inhomogeneity in the physical properties and topology of the electron system, as well as in its dielectric environment.^{10,11}

Nonlocal measurements were conducted to determine the exact position of the rectification of the ac plasmon potential. Potential probes in the form of 2DES narrow $5 \mu\text{m}$ -wide stripes were applied to different parts of the device under investigation. Subsidiary experiments have shown that the probes do not disturb the plasmon potential distribution in the plasmonic resonator. These experiments were conducted in a perpendicular magnetic field. Sufficiently far away from $B = 0$, the plasmon branch, whose frequency decreases with increasing B , may be regarded as edge magnetoplasmon (EMP). Its velocity is proportional to the Hall conductivity $\sigma_{xy} \propto n_s/B$.¹² For the interference of the EMP to occur, q should be an integer multiple of π/L , where L is the total length of the plasmonic resonator. At a fixed density and fixed incident radiation frequency, a B -periodic oscillatory photovoltage is expected with a period

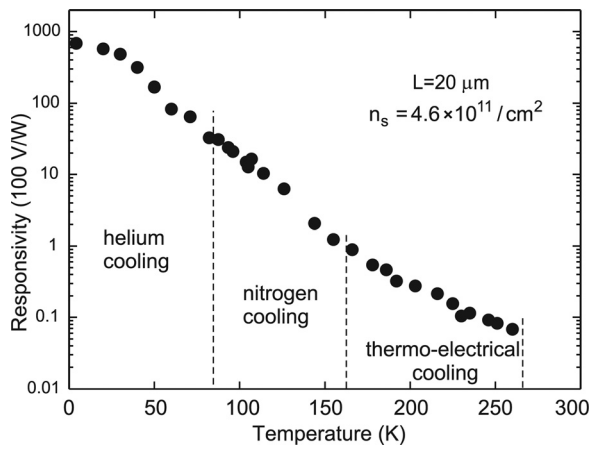


FIG. 3. Temperature dependence of the photovoltage response for a device type B with $L = 20 \mu\text{m}$ and $f = 80 \text{GHz}$. Temperature diapasons of different cooling systems are separated by dashed lines.

of $\Delta B \propto n_s/Lf$. These dependences are indeed confirmed in the experiments (Fig. 2). Figure 2 shows the photovoltage as a function of B , when the 2DES region under G2 is partially depleted to the density $n_1 = 0.5 \times 10^{11} \text{cm}^{-2}$. The measurements were conducted on the type B of structure with $n_s = 1.6 \times 10^{11} \text{cm}^{-2}$ and central plasmonic resonator length $L = 100 \mu\text{m}$. The photovoltage is measured from different pairs of potential probes along the device length. Signals between the probes 3–2, 2–1, and 3–4 are almost zero, indicating that the plasmon rectification near gate G1 does not contribute to the device response. Signals between the probes 5–4 and 6–5 exhibit B-periodic oscillations. The oscillation with period $\Delta B(5-4) \approx 0.3 \text{T}$ corresponds to the EMP interference in the central plasmonic resonator with $L = 100 \mu\text{m}$.⁵ Oscillations with $\Delta B(6-5) = 0.1 \text{T}$ arise from the EMP interference in the plasmonic resonator formed by gate G2 and the source contact ($l = 300 \mu\text{m}$). The data suggest that the rectification of the plasma potential is localized near the density step induced by the potential of gate G2. The inset of Fig. 2 shows that for a plasmonic resonator of length $l = 300 \mu\text{m}$, the plasmon rectification on the contacts is negligible.

Figure 3 displays the temperature dependence of photovoltage measured for the device type B with $L = 20 \mu\text{m}$ at $f = 80 \text{GHz}$ and fixed electron density $n_s = 4.6 \times 10^{11} \text{cm}^{-2}$. The device under study had a rectification defect in the form of an electron density step. Our measurements show that the room-temperature responsivity of the device is equal to 10 V/W. The observed temperature behaviour is determined by two factors. The first factor accounts for temperature depend-

ence of the standing plasma wave amplitude in the plasmonic resonator. The second factor arises from the temperature degradation of the defect rectification efficiency. The amplitude of the plasma wave, which reaches the rectification site, is determined by the ratio of the plasmon coherence length to the resonator length.^{13,14} It was shown that the plasmon coherence length L_p equals $10 \mu\text{m}$ at room temperature for a used high-quality 2DES.¹³ For the device under investigation, the length of the plasmonic resonator (L) was selected as $L = 20 \mu\text{m}$, which is comparable to the plasmon coherence length at room temperature. Our results substantiate the fact that submicron technology is not needed for producing plasmonic devices with embedded rectification defects.

In summary, we have introduced a class of GaAs/AlGaAs quantum well plasmonic on-chip detectors/spectrometers of subterahertz radiation. They can be used for measuring both the frequency and the intensity of radiation at temperatures of up to 300 K. The device operation relies on the excitation of plasma waves by incident radiation with subsequent rectification of the ac plasmon potential by a nonlinear defect. The defect may represent any local inhomogeneity in the physical properties and topology of the 2DES. The device fabrication technology is compatible with standard semiconductor cycles. Therefore, the integration of detectors into a large-scale matrix for use in THz imaging applications does not involve any major difficulty.

¹X.-C. Zhang and J. Xu, *Introduction to THz Wave Photonics* (Springer, New York, 2010).

²M. Dyakonov and M. S. Shur, *Phys. Rev. Lett.* **71**, 2465 (1993).

³M. Dyakonov and M. S. Shur, *IEEE Trans. Electron Devices* **43**, 380 (1996).

⁴W. Knap, M. Dyakonov, D. Coquillat, F. Teppe, N. Dyakonova, J. Usakowski, K. Karpierz, M. Sakowicz, G. Valusis, D. Seliuta *et al.*, *J. Infrared Millim. THz. Waves* **30**, 1319 (2009).

⁵I. V. Kukushkin, M. Yu. Akimov, J. H. Smet, S. A. Mikhailov, K. von Klitzing, I. L. Aleiner, and V. I. Falko, *Phys. Rev. Lett.* **92**, 236803 (2004).

⁶I. V. Kukushkin, S. A. Mikhailov, J. H. Smet, and K. von Klitzing, *Appl. Phys. Lett.* **86**, 044101 (2005).

⁷S. A. Mikhailov and N. A. Savostianova, *Phys. Rev. B* **71**, 035320 (2005).

⁸F. Stern, *Phys. Rev. Lett.* **18**, 546 (1967).

⁹V. M. Muravev, C. Jiang, I. V. Kukushkin, J. H. Smet, V. Umansky, and K. von Klitzing, *Phys. Rev. B* **75**, 193307 (2007).

¹⁰I. V. Kukushkin and V. M. Muravev, U.S. Patent Application 12247096 (7 October 2008).

¹¹V. M. Muravev, I. V. Kukushkin, J. Smet, and K. von Klitzing, *JETP Lett.* **90**, 197 (2009).

¹²V. A. Volkov and S. A. Mikhailov, *Zh. Eksp. Teor. Fiz.* **94**, 217 (1988) [*Sov. Phys. JETP* **67**, 1639 (1988)].

¹³V. M. Muravev, I. V. Kukushkin, A. L. Parakhonskii, J. Smet, and K. von Klitzing, *JETP Lett.* **83**, 246 (2006).

¹⁴V. M. Muravev, I. V. Andreev, I. V. Kukushkin, J. Smet, and K. von Klitzing, *JETP Lett.* **87**, 577 (2008).